CHEMISTRY OF MATERIALS

Article

pubs.acs.org/cm

Organogels and Liquid Crystalline Properties of Amino Acid-Based Dendrons: A Systematic Study on Structure–Property Relationship

Gui-Chao Kuang, Xin-Ru Jia,* Ming-Jun Teng, Er-Qiang Chen,* Wu-Song Li, and Yan Ji

Beijing National Laboratory for Molecular Sciences and Key Laboratory of Polymer Chemistry and Physics of the Ministry of Education, College of Chemistry and Molecular Engineering, Peking University, Beijing, China 100871

Supporting Information

ABSTRACT: Self-assembly behaviors of a series of amino acids-based dendrons, from the first generation (G1) to the third generation (G3) with various focal moieties or peripheral groups, were systematically studied. The supramolecular structures in organogels, thermotropic and lyotropic liquid crystals (LCs) were measured. The influence of the focal groups, dendritic branches, and generation numbers on the mesophase of organogels or LCs was studied by a combination of experimental techniques including transmission electronic spectrometry (TEM), atomic force microscopy (AFM), infrared (IR) spectra, wide-angle X-ray diffraction (WAXD), and small-angle X-ray scattering (SAXS). It was found that the gelation ability of the dendrons in organic solvents was highly related to the generation; namely, none of the G1 dendrons could form organogels, G2 dendrons displayed good gelation ability, and G3 dendrons gelled the organic solvents with the lowest critical gelation concentration. Oscillatory shear measurements indicated that the gels behaved as viscoelastic materials with good tolerance to external shear force. In addition, all of G3 dendrons and some G2 dendrons were capable of self-organizing to afford the thermotropic and lyotropic LCs.

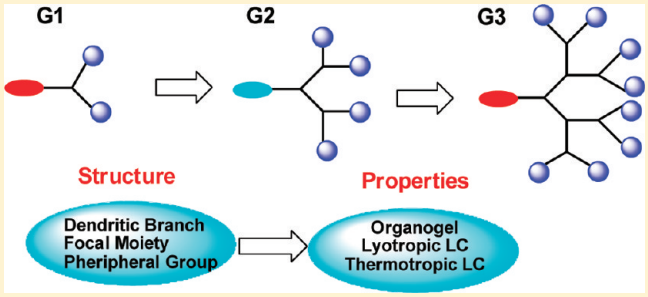

KEYWORDS: *amino acids, dendrons, self-assembly, organogel, thermotropic and lyotropic liquid crystal*

INTRODUCTION

Considerable effort has been made to advance our knowledge of the soft materials of polypeptide-based dendritic molecules, such as organogels and liquid crystals (LCs), since the inspiration from the pioneering works by Aida,[1] Smith,[2] and Percec.[3] More and more synthetic dendritic compounds acting as organogelators have been reported, which enriches the soft materials and enlarges the view boundary of researchers.[4] Amino acids-based dendritic gelators have aroused particularly increasing interest due to their broad structural diversities and potential biomedical applications. Dendritic gelators from various amino acids, including lysine,[5] L-glutamate acid,[6] L-aspartic acid,[7] and ornithine,[8] etc., have been documented. Intriguing findings are convinced that the focal group,[1] chiral center,[9] and generations[10] have pronounced effects on the self-assembly process. Furthermore, the amino acid layer sequence shows huge influence on the gelation properties.[11]

On the other hand, investigation of the LC properties of dendritic compounds is also a current topic for their potential applications in functional materials.[12] As two kinds of LC, thermotropic LCs (occurring by heating) and lyotropic LCs (induced by isotropic solvents) show strict differentiation depending on the molecular shape and structures. Most reported materials exhibiting both thermotropic and lyotropic LCs are amphiphilic compounds.[13] As to dendritic molecules, LC properties can be endowed with dedicated structural designs of molecules at the focal point, in dendritic branches, and on peripheral moieties. A series of amphiphilic twin-dendritic compounds behaving as thixotropic organogel in solution and thermotropic LC in bulk have been investigated.[14] However, it is not common for dendritic molecules to behave simultaneously as organogels and lyotropic and thermotropic LCs, owing to the subtle relationship between the intrinsic units and supermolecular structures. Up to now, polypeptide-based dendrons with both gel and LC properties have been rarely reported. Although Kato et al. have revealed that a dendritic oligopeptide containing the pyrene focal group displayed both gel and LC properties, the hexagonal columnar LC mesophase was observed by addition of 2,4,7-trinitrofluorenone (TNF), which can increase intermolecular force by donor–acceptor interaction.[15] It is anticipated that the elucidation of the principles of the self-assembly process of gel and LC will allow the development of a variety of biologically inspired systems.[16]

We initiated a research program to address the versatile self-assembly properties of glycine/L-aspartic acid dendrons in organic solvents in 2005.[17] It is found that the third generation (G3) dendron displays not only effective organogel but also lyotropic LC in benzyl alcohol. On the basis of our understanding of hydrogen bonding and $\pi-\pi$ stacking working in concert to regulate the supramolecular assembly and solvent-dendron

Received: July 5, 2011
Revised: November 18, 2011
Published: December 19, 2011

interaction required for lyotropic LC property, we have enabled significant advances in designing polypeptide dendritic molecules to show organogel, lyotropic, and even thermotropic LC properties.[18] In implementing our previous studies, photoresponsibility of dendrons focally modified with *azo* and *cinnamate* groups also have been investigated.[19]

Herein, we describe systematically the self-assembly properties of dendrons with different amino acid combinations as building blocks, including glycine and L-aspartic acid (gly−asp), glycine and L-glutamic acids (gly−glu), and D-alanine and L-aspartic acid (ala−asp). Both their gel and LC properties were systematically investigated and compared in detail. Some fundamental molecular parameters, for design principles, to regulate the supramolecular structures also have been revealed by changing the structure of the focal moieties, dendritic branches, generation numbers, and peripheral groups.

RESULTS AND DISCUSSION

Molecular Design and Synthesis. In our studies, different amino acids-based dendrons with generations 1−3 that consisted of glycine/L-aspartic acid (gly−asp), glycine/L-glutamic acids (gly−glu), and D-alanine/L-aspartic acid (ala−asp) were convergently synthesized (Scheme 1) and further modified, either on

Scheme 1. Convergent Synthesis of the Different Generations of Dendrons Boc-G*n* (*n* = 1, 2, and 3)[a]

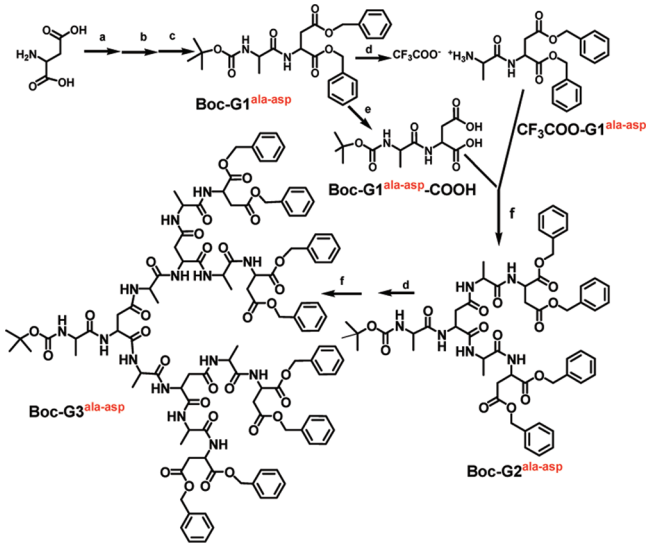

[a]Reagents and conditions: (a) *p*-toluenesulfonic acid, benzene, benzyl alcohol, refluxing; (b) CH_3OH, KOH; (c) Boc-D-alanine, DCC, −10 °C; (d) TFA, CH_2Cl_2; (e) Pd−C, H_2, ethanol; and (f) DCC, Boc-G1$^{ala-asp}$-COOH, *N*-methylmorpholine, NHS, −10 °C. Boc = *tert*-butoxycarbonyl, DCC = dicyclohexylcarbodiimide, TFA = trifluoroacetic acid, NHS = *N*-hydroxy-succinimide. ala−asp: D-alanine and L-aspartic acid.

the periphery or at the focal point. Scheme 2 summarizes the total of 23 dendritic molecules we synthesized. The detailed synthetic procedures for partial dendrons have been previously reported (Supporting Information).[17,18a,b,d] As a representative, Scheme 1 depicts the general procedures involved in the synthesis of D-alanine and L-aspartic acids-based dendrons. The standard DCC coupling of Boc-D-alanine and benzyl protected L-aspartic acid generated the first generation (G1) of the dendron. The second (G2) and third generations (G3) were synthesized by repeating two-reaction cycle, that is, by removing the Boc group of the lower-generation dendron with trifluoroacetic acid (TFA) and then coupling the resultant N-deprotected intermediate to the C-deprotected G1 (Boc-G1-COOH), which was prepared by hydrogenative debenzylation of the dipeptide. The synthetic procedures of dendrons referred to this article have been reported previously,[17,18a,b,d] with the exception of Acrylic-G2$^{ala-asp}$ and Boc-G3$^{ala-asp}$, which are described in the Supporting Information.

Organogelation Behavior. To avoid evaporation of the liquid components, gels were prepared in a sealed vial (i.d. ≈ 1 cm).

Scheme 2. Structures of G1, G2, and G3 Dendrons

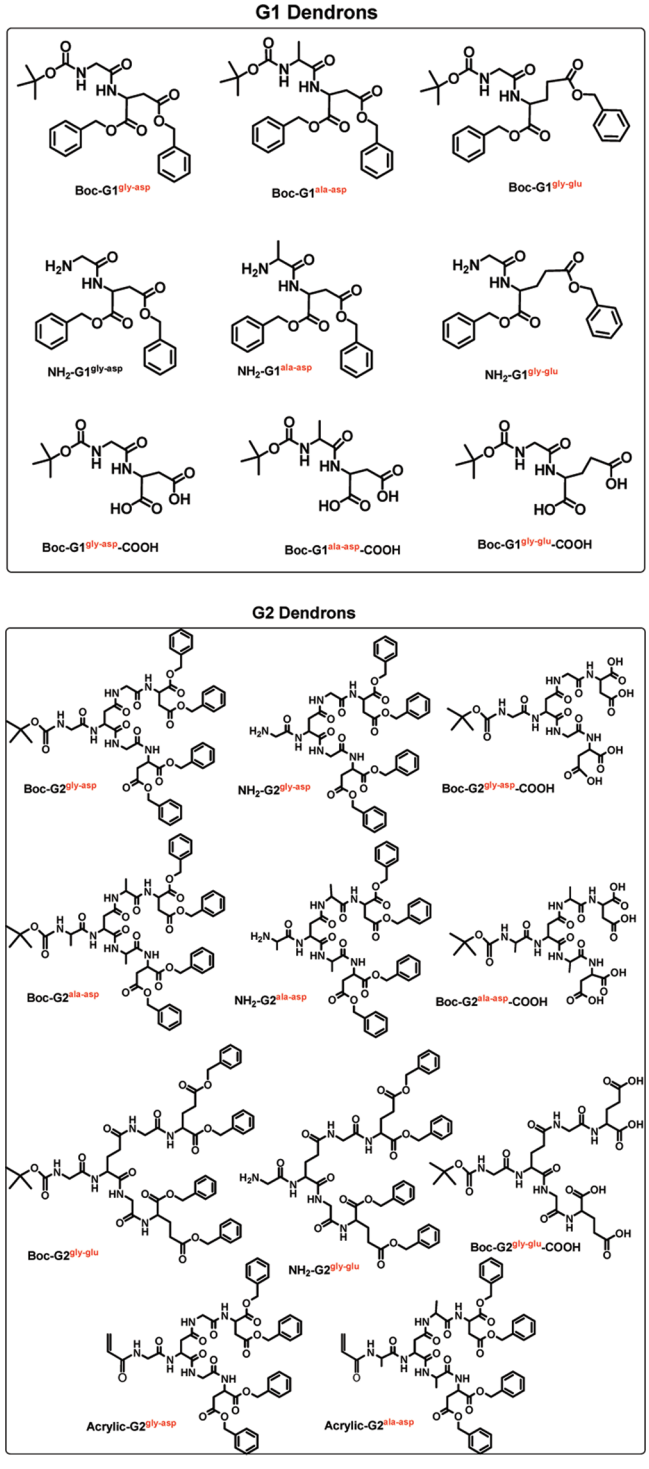

dx.doi.org/10.1021/cm201913p | *Chem. Mater.* 2012, 24, 71−80

Scheme 2. continued

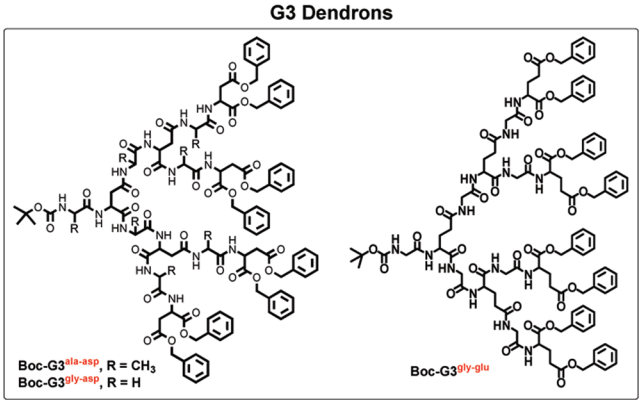

Weighed quantities of dendritic gelator and liquid were heated to obtain a homogeneous solution. Then, the vial was placed under room temperature (25 °C) for 1 h. If the cooled samples were not visually phase-separated and did not flow perceptibly when the vials were inverted, they were considered to be gels. Ultrasound, as another alternative for gel preparation, has gained more attention.[20] Here, the gelation of Boc-G2$^{ala-asp}$ in 1,2-dichloroethane (DCE) was observed exclusively under ultrasound, while only precipitate could be afforded without sonication. The gelation ability of the dendrons is summarized in Table 1. Through the systematic studies on the gelation of the obtained compounds, some structural factors essential for the fibrous assembly can be summarized. First, the dendrons with higher generation show lower critical gelation concentration (CGC). All of the G1 dendrons cannot gel any solvent we used, while G2 dendrons form gel with similar CGC values regardless of the amino acids branches, and the gels from G3 dendrons have the lowest CGC values, which is probably attributed to more hydrogen-bonding sites from the amide groups. Such dendritic effect is consistent with the results in Smith's reports.[21] Second, all of Boc-G2-COOH dendrons, without benzyl groups on the periphery, cannot form gel in common solvents, indicating the indispensability of $\pi-\pi$ stacking between the phenyl moieties. Detailed mechanistic and theoretical studies by Smith's group demonstrated that benzyl groups would enhance the enthalpic contribution between dendritic molecules and lead higher degree organization.[22] Third, Boc-G2$^{ala-asp}$ dendrons exhibit excellent gelation ability in methanol and 1,2-dichloroethane (DCE), while both Boc-G2$^{gly-asp}$ and Boc-G2$^{gly-glu}$ show good solubility in these solvents. We are not sure at this point why Boc-G2$^{ala-asp}$ behaves as the best gelator; we speculate that the stereogenic center of alanine may be responsible for better gelation or the additional methyl groups may provide additional hydrophobic interaction to increase the dendron's solubility.[23] Finally, G2 dendrons with amine and acrylic as the focal groups have stronger gelation tendency than other G2 dendrons because of their smaller steric hindrance. For example, Acrylic-G2$^{gly-asp}$ could gel more organic solvents at a very low concentration (e.g., 4 mg/mL in THF) as compared with Boc-G2$^{gly-asp}$.[18b]

Sol–Gel Phase Transition Temperature. To further evaluate the dendritic effect and focal moiety on the thermal stability of the gel, the gel–sol transition temperatures (T_{gel}) of Boc-G2$^{ala-asp}$, Acrylic-G2$^{ala-asp}$, and Boc-G3 $^{ala-asp}$ in 1,2-dichloroethane were compared under different concentrations and the results are shown in Figure 1. As expected, the T_{gel} values increased with the concentration increasing, and then reached maximum and remained almost constant thereafter.

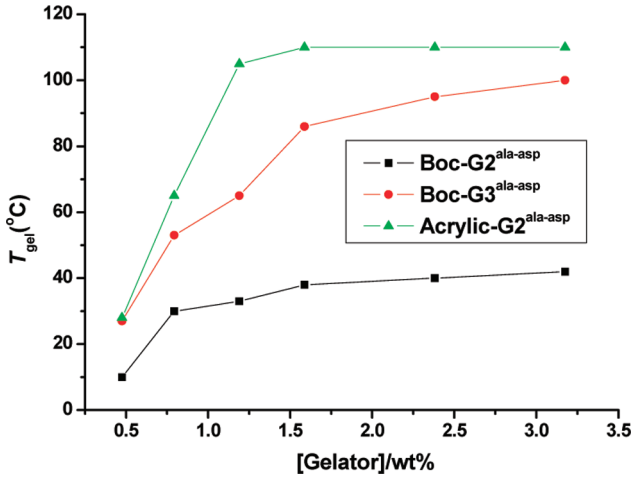

Figure 1. Plots of T_{gel} against the concentration of Boc-G2$^{ala-asp}$, Acrylic-G2$^{ala-asp}$, and Boc-G3$^{ala-asp}$ in 1,2-dichloroethane with the heating rate 1 °C/min in oil bath.

Table 1. Organogelation Abilities of the Dendrons[a]

solvents	G1	Boc-G2$^{ala-asp}$	Boc-G2$^{gly-glu}$	Boc-G2$^{gly-asp}$	Acrylic-G2$^{ala-asp}$	Acrylic-G2$^{gly-asp}$	H_2N-G2$^{ala-asp}$	Boc-G3$^{ala-asp}$	Boc-G3$^{gly-glu}$	Boc-G3$^{gly-asp}$	Boc-G2-COOH
$CHCl_3$	S	S	S	S	G(6)	G(5)	G(6)	G(9)	G(22)	G(13)	P
CH_3OH	S	G(30)	S	S	G(5)	G(6)	G(7)	G(11)	G(4)	G(7)	S
EtOH	S	G(27)	G(18)	S	G(9)	G(7)	G(13)	G(14)	G(16)	G(5)	S
EtOAc	S	G(15)	G(50)	G(22)	G(7)	G(10)	G(17)	G(5)	G(13)	G(7)	S
THF	S	S	S	S	G(5)	G(4)	G(8)	G(6)	G (15)	G(5)	S
benzene	S	G(7)	G(6)	G(6)	G(6)	G(8)	G(4)	G(2)	G(3)	G(6)	P
toluene	S	G(11)	G(10)	G(10)	G(4)	G(6)	G(5)	G(1)	G(2)	G(3)	P
acetone	S	PG	S	PG	G(5)	G(8)	PG	G(2)	G(4)	G(4)	S
DCE	S	G(10)	S	S	G(7)	G(5)	G(3)	G(6)	G(8)	G(12)	P
cyclohexane	S	P	P	PG	PG	PG	PG	P	P	P	P
DMSO	S	S	S	S	S	S	S	S	S	S	S
DMF	S	S	S	S	S	S	S	S	S	S	S
H_2O	P	P	P	P	P	P	P	P	P	P	S

[a]: P, precipitate; PG, partial gel; G, gels, S, soluble (>100 mg mL^{-1}). The values given in parentheses are the minimum concentration (mg mL^{-1}) to achieve gelation at 25 °C.

dx.doi.org/10.1021/cm201913p | *Chem. Mater.* 2012, 24, 71–80

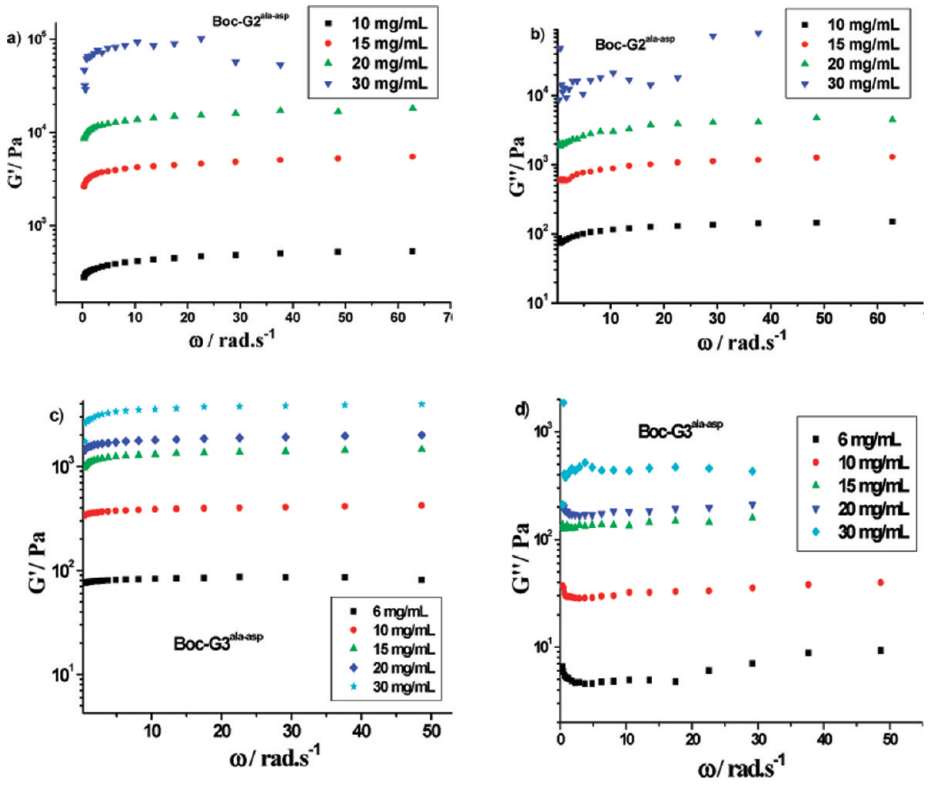

Figure 2. Dynamic moduli, G′ and G″ vs angular frequency on double logarithmic scale for dendrons Boc-G2$^{ala-asp}$ and Boc-G3$^{ala-asp}$ gels at different concentrations in 1,2-dichloroethane at 25 °C. Stress amplitude 0.1 Pa.

On the other hand, the T_{gel} values of Boc-G3$^{ala-asp}$ are higher than those of Boc-G2$^{ala-asp}$ at the same concentration. The same trend was also observed for the dendrons with the glycine/L-glutamic acid (gly−glu) and glycine/L-aspartic acids (gly−asp) as the building blocks. From the architectural point of view, the intermolecular interactions of the Boc-G3$^{ala-asp}$ might be stronger than those of the Boc-G2 $^{ala-asp}$ because of more amide groups in the dendritic branches, which can lead to more thermally stable supramolecular organogels. Moreover, it was found that the T_{gel} values of Acrylic-G2$^{ala-asp}$ gels were about 20−60 °C higher than those of Boc-G2$^{ala-asp}$ gels (concentration from 0.5 to 3.2 wt %), which might be attributed to the focal acrylic group that can reduce the steric hindrance and provide more $\pi-\pi$ interaction, as compared to the focal Boc moiety. This observation indicates that a minor structural difference in the molecules can affect the property greatly.

Rheological Properties. To assess the dynamic nature and relaxation modes of Boc-G2$^{ala-asp}$ and Boc-G3$^{ala-asp}$ gels in 1,2-dichloroethane (DCE), the oscillatory shear measurement was conducted (Figure 2). Data was collected by using a stress-controlled rheometer with parallel plate-type geometry, as a function of angular frequency from 70 to 0.1 rad/s, by using a stress-controlled rheometer with parallel plate-type geometry. Both the storage modulus (G′) and the loss modulus (G″) of Boc-G2$^{ala-asp}$ and Boc-G3$^{ala-asp}$ exhibit slight frequency dependence, with G′ an order of magnitude larger than G″, implying that the gels are a typical elastic rather than viscous soft matter. It is worth mentioning that the storage modulus of Boc-G2$^{ala-asp}$ gel is obviously larger than that of Boc-G3$^{ala-asp}$, indicating that the gel from Boc-G2$^{ala-asp}$ is more rigidity associated with the elastic gel structure. However, the detailed reason for the observed modulus increasing of Boc-G2$^{ala-asp}$ organogel is not clear at present.

It is common sense that the gels are highly sensitive to external force; that is, gels will yield or flow under an applied stress.[24] In this work, the mechanical properties measurements of Boc-G2$^{ala-asp}$ and Boc-G3$^{ala-asp}$ gels at different concentrations were performed (Figure 3). Both G′ and G″ showed a wide plateau region until the strain amplitude reached one critical stress value known as the yield value. After exceeding this value, they started to drop dramatically. This should be due to the partial collapse of the gels. This observation is consistent with universally accepted results that a gel is prone to show a viscous response under long time scales (low frequencies), and it also agrees well with the studies that the gels show relaxation processes at shorter time scales (high frequencies). Apparently, comparison of the yield values of the gels demonstrates that the G′ and G″ of Boc-G2$^{ala-asp}$ gel are obviously larger than those of Boc-G3$^{ala-asp}$ at the same concentration. These results are well consistent with the results of viscoelasticity tests, as mentioned above.

Driving Force Analysis. The cooperation of hydrogen bonding and $\pi-\pi$ stacking are considered as the major driving forces responsible for the fibrous aggregates. As demonstrated in our previous report, the $\pi-\pi$ stacking between the phenyl rings can be proved by pyrene probe, whose emission intensity ratio I_1/I_3 is an indicator for the polarity of microenvironment.[17,18] For example, it was found that the I_1/I_3 ratio of pyrene decreased gradually with increasing the concentration of Boc-G3$^{gly-asp}$ and Boc-G3$^{gly-glu}$, which indicates the formation of a nonpolar microenvironment by virtue of the $\pi-\pi$ stacking of the peripheral phenyl groups.

To clarify the existence of hydrogen bonding, temperature and concentration-dependent ^{1}H NMR experiments were performed. Taking Boc-G3$^{gly-glu}$ gel (13 mg/mL in $CDCl_3$) as an example, the signals at 8.49 and 5.72 ppm due to the protons of

dx.doi.org/10.1021/cm201913p | Chem. Mater. 2012, 24, 71−80

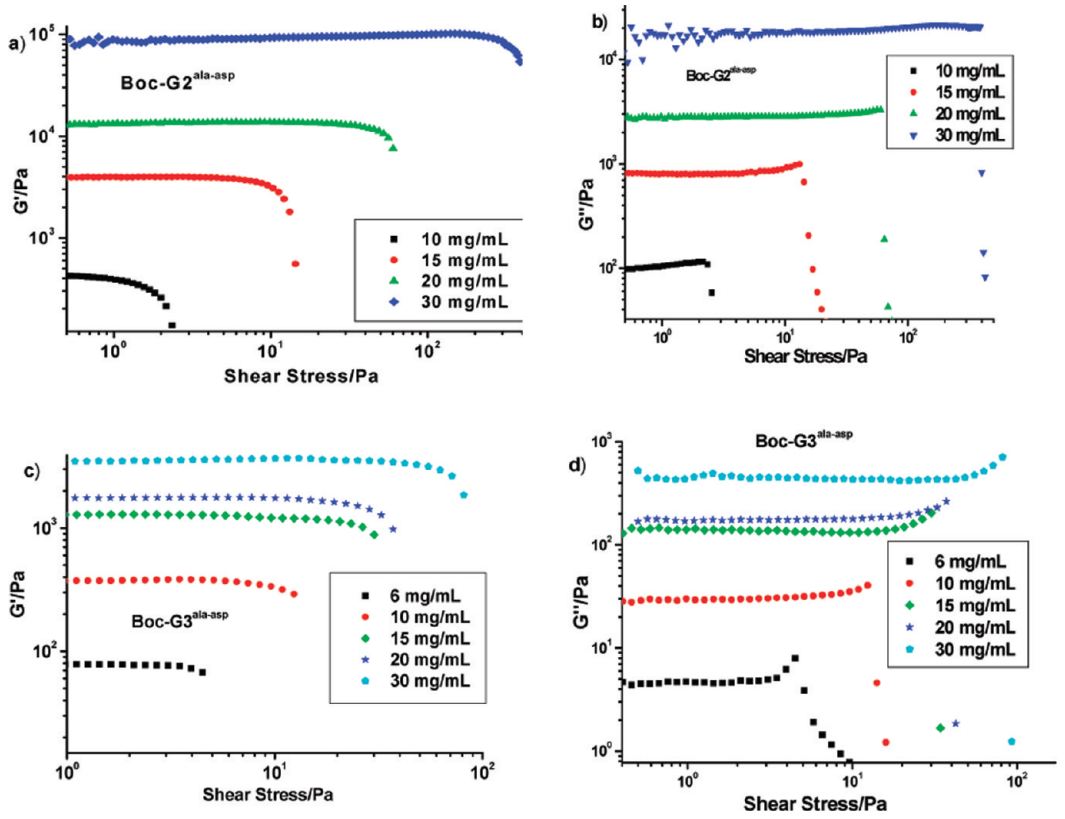

Figure 3. Storage modulus G′ and loss modulus G″ (1 rad/s) for dendrons Boc-G2$^{ala-asp}$ and Boc-G3$^{ala-asp}$ gels as a function of imposed stress in 1,2-dichloroethane at 25 °C.

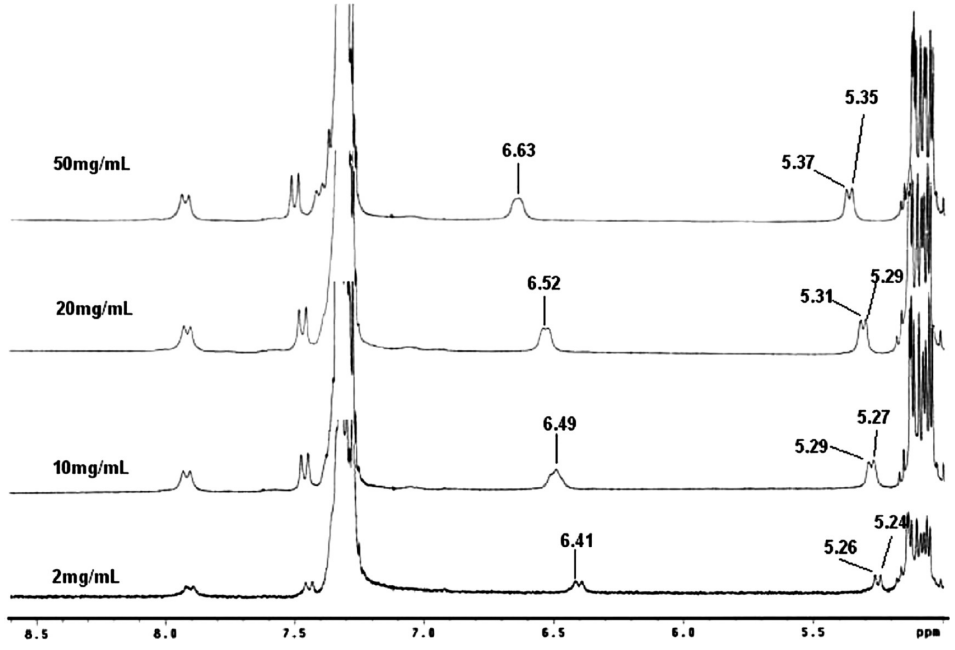

Figure 4. ^{1}H NMR spectra of Boc-G2$^{ala-asp}$ in $CDCl_3$ at 2, 10, 20, 50 mg mL^{-1} at 25 °C.

amide groups were gradually upfield shifted to 8.10 and 5.66 ppm with increasing temperatures from 24 to 55 °C.[18a] Moreover, the ^{1}H NMR spectra of Boc-G2$^{ala-asp}$ were recorded at different concentrations (Figure 4). By increasing the concentration from 2 to 50 mg/mL, the signals at 5.24, 5.26, and 6.41 ppm ascribed to the amide moieties are gradually downfield shifted to 5.35, 5.37, and 6.63 ppm, respectively. These results strongly demonstrate the progressive involvement of these groups in hydrogen bonding.[25]

FTIR is another powerful tool for investigating organogels because it can measure the sample either in the gel state or in the sol state. To further confirm the hydrogen bonding interaction, the FTIR spectra of Boc-G2 (Boc-G2$^{ala-asp}$, Boc-G2$^{gly-glu}$, and Boc-G2$^{gly-asp}$) and Boc-G3 (Boc-G3$^{ala-asp}$, Boc-G3$^{gly-glu}$,

dx.doi.org/10.1021/cm201913p | Chem. Mater. 2012, 24, 71–80

and Boc-G3$^{gly-asp}$) both in solution and gel state were recorded (Figure 5). It is found that the solution of Boc-G2$^{gly-glu}$ displays

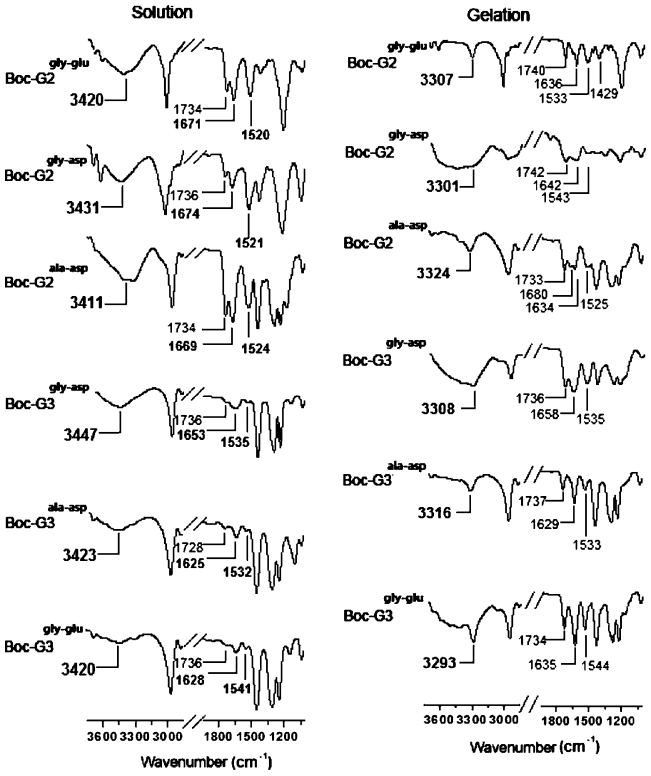

Figure 5. IR spectra of second and third generation dendrons in solution and gelation states.

the signals at 3420, 1671, and 1520 cm^{-1} assigned to N−H bending vibrations, amide I, and II bands, respectively, evidencing no hydrogen bonding in its sol state.[26] For Boc-G3$^{ala-asp}$ dendron in sol state, the FTIR spectrum shows different information from Boc-G2$^{gly-glu}$; namely, the predominating amide I and II bands shifted to 1625 and 1532 cm^{-1} and a shoulder peak appeared around 3423 cm^{-1}, which indicate the intramolecular hydrogen bonding interaction and free NHs when the molecules are in the solution.[27] However, the FTIR spectra of the corresponding gels present different characters; namely, the signals ascribed to N−H bending vibrations shift to lower wavenumbers with a 100 cm^{-1} frequency in 1,2-dichloroethane; the amide I and II bands of Boc-G3$^{ala-asp}$ and Boc-G3$^{gly-glu}$ gels shift to 1629, 1533 cm^{-1} and 1635, 1544 cm^{-1}, with the exception of the amide I band signal of Boc-G3$^{gly-asp}$ gel, which appears at a higher wavenumber of 1658 cm^{-1}, indicating the existence of both the intra- and intermolecular hydrogen bonding interactions.

Morphologies and Architectures of Organogels. To gain better insight into the molecular organization, the xerogels were examined by atomic force microscopy (AFM) and transmission electron microscopy (TEM). As shown in Figures 6 and 7, all the xerogels exhibited highly developed and intertwined fibrous networks, suggesting a great extent of supramolecular aggregates. The fibers showed a large aspect ratio (length over width), with several micrometers in length and approximately 30 nm in width. TEM images show that the fiber density of Boc-G2$^{ala-asp}$ gel is higher than that of Boc-G3$^{ala-asp}$ gel, which is consistent with our rheological observation. It is worth mentioning that, in the case of Boc-G2$^{ala-asp}$ xerogel, a

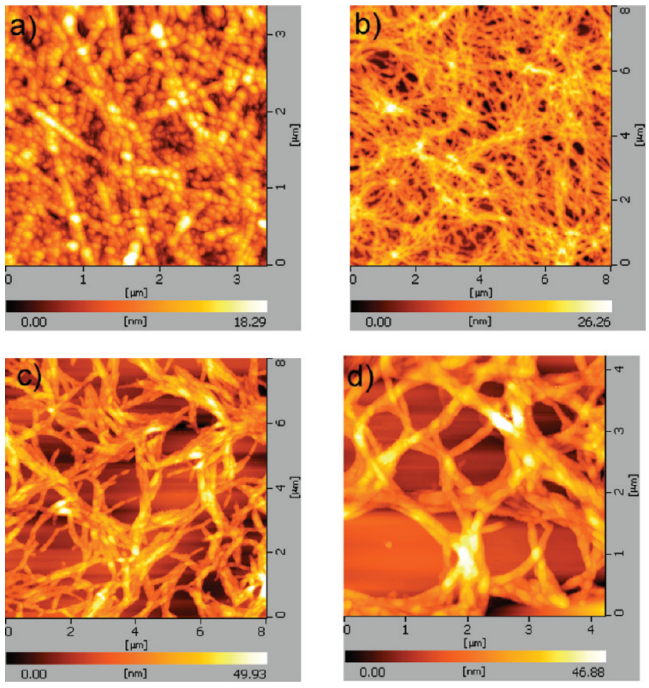

Figure 6. AFM images of (a) Boc-G2$^{ala-asp}$, (b) NH_2-G2$^{ala-asp}$, (c and d) Boc-G3$^{ala-asp}$ with different magnifications in 1,2-dichloroethane.

series of bead-like fibers were observed, which might be owing to the chiral center of D-alanine. However, it is difficult to make certain whether they are helices or not.[28] Of interest for the case of Boc-G3$^{gly-asp}$ and Boc-G3$^{ala-asp}$ gels, the magnified images further visualize thinner fibril structures in the fiber bundles, indicating a hierarchical self-assembly process.

It has been well-developed by Smith et al. that the properties and morphologies of two-component gels can be easily modulated by changing their molar ratio.[29] Inspired by their excellent work, we expected to observe the deferent morphologies of two components gels from Boc-G1$^{ala-asp}$-COOH and NH_2-G2$^{ala-asp}$. Figure 8 presents the AFM images of dried gels prepared from methanol with different molar ratios of Boc-G1$^{ala-asp}$-COOH and NH_2-G2$^{ala-asp}$. In the case of the gel of NH_2-G2$^{ala-asp}$ and Boc-G1$^{ala-asp}$-COOH with the molar ratio of 1:1, one-dimensional fibers with helix-like structure are observed (Figure 8b). A similar morphology of Boc-G2$^{ala-asp}$ xerogel has also been observed in our previous observations. Although we cannot ascertain that the fibers are really helical or not, we suppose that the chiral center in the structure of D-alanine might endow the assemblies with helix conformation. When the molar ratio changed to 1:5, the morphology of the gel becomes a mess and no regular fiber can be found. According to the report by Smith et al.,[29] in such a case, the fibers from two components connected to each other in three dimensions, leading the gel phase to be developed in a cubic way because more carboxyl groups were involved. Additionally, the average height of the fibers increased from 20 nm for NH_2-G2$^{ala-asp}$ (5 mg/mL) alone to 50 nm (molar ratio 1:1) after adding Boc-G1$^{ala-asp}$-COOH and then to several hundred nanometers with the ratio of 1:5, which is well consistent with the results of two-component lysine dendritic gels (Figure 8d and e).[30]

The packing patterns of a series of xerogels made up of the self-assembled fibers from the G2 and G3 dendrons with different amino acids as components were examined by wide-angle X-ray diffraction (WAXD) and small-angle X-ray scattering (SAXS).

dx.doi.org/10.1021/cm201913p | Chem. Mater. 2012, 24, 71−80

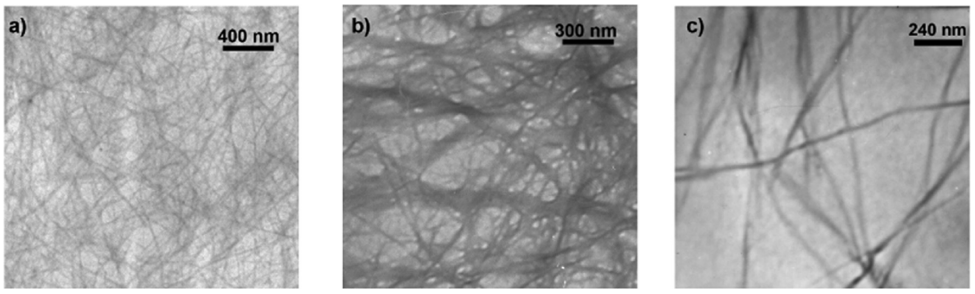

Figure 7. TEM images of (a) Boc-G2$^{ala-asp}$, (b) NH_2-G2$^{ala-asp}$, and (c) Boc-G3$^{ala-asp}$ xerogels made in 1,2-dichloroethane.

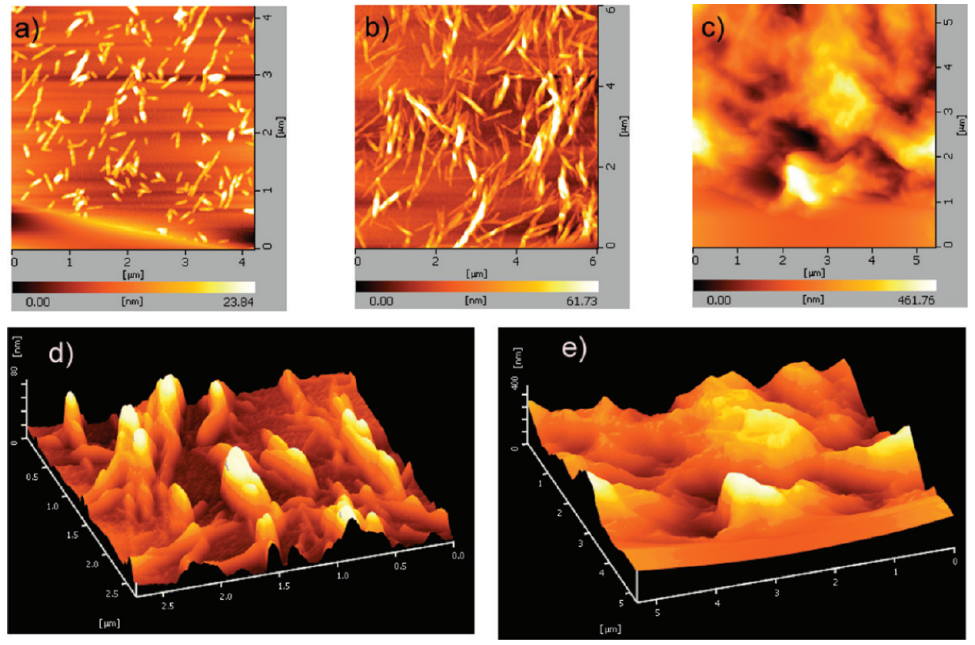

Figure 8. AFM images of xerogel of NH_2-G2$^{ala-asp}$ and Boc-G1$^{ala-asp}$-COOH mixture in methanol in a ratio of (a) 1:0, (b and d) 1:1, (c and e) 1:5.

It reconfirmed that small changes in the structures of the gelators result in dramatic changes in the aggregation mode.

As shown in Figure 9a and b, both Boc-G2$^{gly-asp}$ and Boc-G2$^{gly-glu}$ self-organized into lamellar architecture, with the layer thickness of 3.20 and 3.55 nm, respectively. On the basis of CPK molecular calculation, we can assume that each of the lamella consist of two layers of partially interdigitated two dendrons. In great contrast to Boc-G2$^{gly-asp}$ and Boc-G2$^{gly-glu}$, when the glycine is replaced by D-alanine in the dendritic branches, the Boc-G2$^{ala-asp}$ xerogel displays a hexagonal lattice, with an intercolumnar distance of 5.70 nm. Contrary to the lamellar architecture of Boc-G3$^{gly-asp}$ and Boc-G3$^{gly-glu}$ xerogels, the scattering pattern of Boc-G3$^{ala-asp}$ is essentially different. The SAXS patterns recorded numerous reflections, with the first two peaks at 2.51 and 1.78 nm in the low angle region (Figure 9f). These scattering peaks can be assigned to be Miller indices (10), (11), respectively, of a columnar centered rectangular lattice with a = 4.96 nm and b = 5.52 nm.

The focal group tremendously affected the packing mode of the gel phase. For example, replacing the focal Boc by an amine unit, the WAXD pattern of the corresponding NH_2-G2$^{ala-asp}$ xerogels showed two peaks appearing at 3.83 and 1.45 nm in the low angle region, indicating the structural transition from a hexagonal columnar arrangement to a rectangular lattice. In addition, when the focal point is modified with an acrylic group, Acrylic-G2$^{ala-asp}$ xerogel displays a columnar hexagonal phase.

Liquid Crystalline Properties. The molecular shape with a high aspect ratio is a crucial prerequisite to form LC mesophase. Percec et al. have extended this idea to the dendrimers/dendrons field.[31] Our entry into the field of LCs was rather serendipitous. Occasionally, we found dendron Boc-G3$^{gly-asp}$ self-organized into lyotropic nematic LCs in benzyl alcohol.[17] Following this, we launched an extensive study on the LC properties of natural amino acids-based dendrons, from which the result was convincing that a small structural change of the dendrons also had a huge impact on their LC behaviors.[18b] We have now undertaken systematic studies on the LC properties of related dendrons and made an effort to formulate a structure−property correlation. Herein, we essentially attempt to address the major structural issues by using a combination of techniques including SAXS, WAXD, polarized light microscopy (PLM), and differential scanning calorimetry (DSC).

The dendritic effect related with the LC development is observed. The high generation dendrons facilitated to form LC mesophase, but none of the G1 dendrons studied here displayed thermotropic and lyotropic LCs. The G2 dendrons, such as Boc-G2$^{ala-asp}$, are capable of forming thermotropic LCs. After cooling the sample from isotropic fluid state, birefringent

dx.doi.org/10.1021/cm201913p | *Chem. Mater.* 2012, 24, 71−80

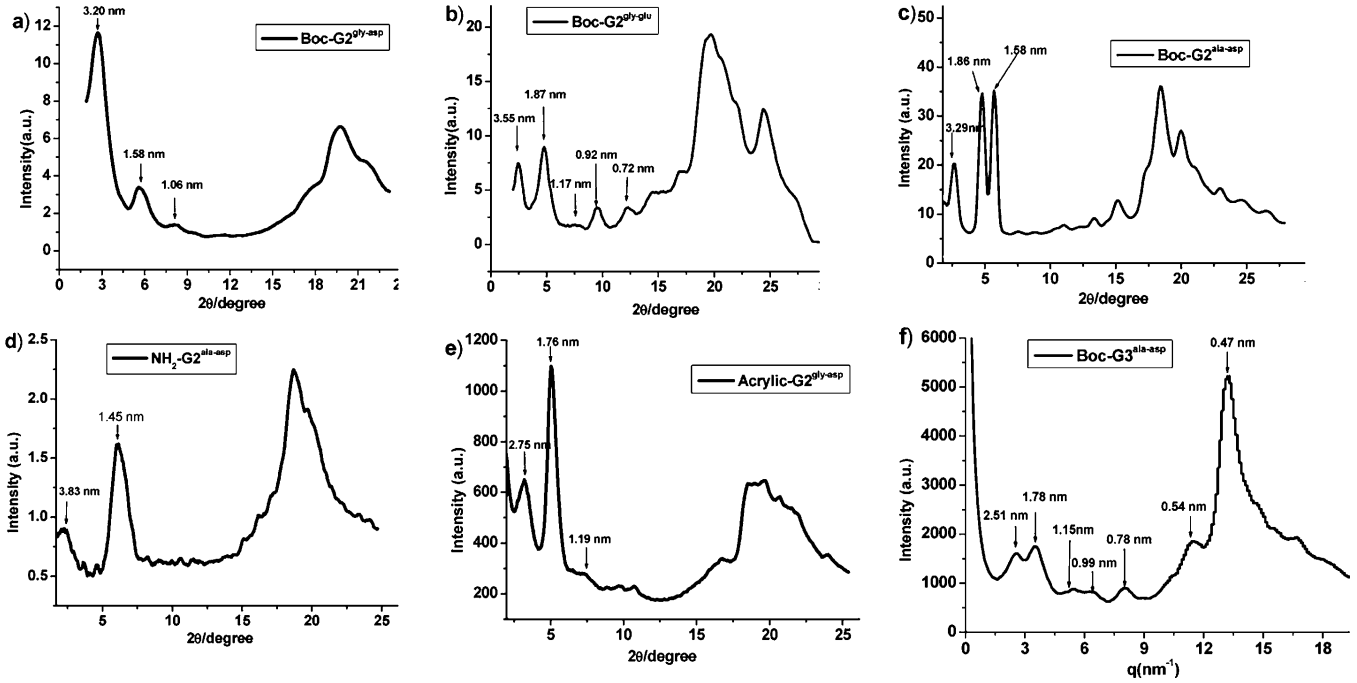

Figure 9. WAXD patterns of xerogel (a) Boc-G2$^{gly-asp}$ made from benzene,[18b] (b) Boc-G2$^{gly-glu}$ made from ethyl acetate,[18a] (c) Boc-G2$^{ala-asp}$ made from 1,2-dichloroethane by ultrasound, (d) NH_2-G2$^{ala-asp}$ made from chloroform, and (e) Acrylic-G2$^{gly-asp}$ made from THF. (f) SAXS of Boc-G3$^{ala-asp}$ made from chloroform.

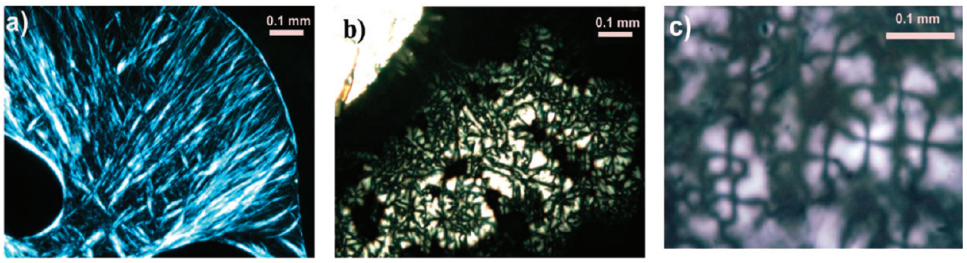

Figure 10. PLM images of (a) Boc-G2$^{ala-asp}$ at 150 °C, (b) Acrylic-G2$^{gly-asp}$ at 100 °C,[18b] and (c) Acrylic-G2$^{ala-asp}$ at 180 °C.

and thread textures were observed under PLM (Figure 10a). Various temperature SAXS/WAXD measurements of Boc-G2$^{ala-asp}$ at various temperatures were performed to identify the mesophase structures. At 110 °C, the pattern shows diffraction peaks at 4.41, 2.20, and 1.52 nm, with a sharp peak centered at 0.48 nm in the wide angle region (Figure S1 in the Supporting Information). The *q*-ratio of 1:2:3 confirmed that the mesophase possessed an arrangement of a lamellar structure. In addition, a shoulder peak at 1.44 nm and the sharp peak at 0.48 nm indicated the existence of some sort of highly ordered molecular packing. All Boc-G3 dendrons (including Boc-G3$^{gly-asp}$, Boc-G3$^{gly-glu}$, and Boc-G3$^{ala-asp}$) not only performed as efficient organogelators but also self-organized into lyotropic LCs in benzyl alcohol with either spherulites or oily streak textures (Figure 11d–f). DSC experiments revealed that only one transition temperature appeared at low concentrations in the cooling process, implying only one lyotropic LC phase (Figure S4 in the Supporting Information). The tendency of taking a lamellar phase for the dendrons Boc-G3$^{ala-asp}$ and Boc-G3$^{gly-glu}$ on cooling is consistent with the results from amino acid-based dendrons described previously (Figure 12).[17]

Regarding the LC properties, there are a few points worthy of note. (1) The thermotropic LC properties of G2 dendrons significantly depended on the building blocks. For example, neither Boc-G2$^{gly-asp}$ nor Boc-G2$^{gly-glu}$ could self-organize into mesophase architecture. (2) The nature of the LC behavior of the dendrons is directly correlated with the focal groups. When the Boc group was removed, none of NH_2-G2 dendrons (including NH_2-G2$^{ala-asp}$, NH_2-G2$^{gly-asp}$, and NH_2-G2$^{gly-glu}$) presented LC properties. However, both Acrylic-G2$^{gly-asp}$ and Acrylic-G2$^{ala-asp}$, with an acrylic group at focal point, formed thermotropic LCs after cooling the samples from isotopic state. For example, an exothermic peak of LC phase transition was observed for Acrylic-G2$^{ala-asp}$ at 205 °C in the cooling traces (Figure S3 in the Supporting Information). We presume that the acrylic moieties favor $\pi-\pi$ stacking and depress the steric hindrance, which facilitates the formation of LCs.[18b] The focal conic fan texture for both Acrylic-G2$^{gly-asp}$ and Acrylic-G2$^{ala-asp}$ is observed by PLM, as shown in Figure 10b and c. The SAXS diagram of Acrylic-G2$^{gly-asp}$ (recorded at 90 °C) revealed a columnar hexagonal phase deduced from the diffractions with a *q*-ratio of 1:$\sqrt{3}$. In contrast, when glycine was replaced by D-alanine in the structure of Acrylic-G2$^{ala-asp}$, the lamellar packing pattern was observed in its LC phase (Figure S1b in the Supporting Information). (3) The amino acid components of dendrons are an important parameter in the LC phase

dx.doi.org/10.1021/cm201913p | *Chem. Mater.* 2012, 24, 71–80

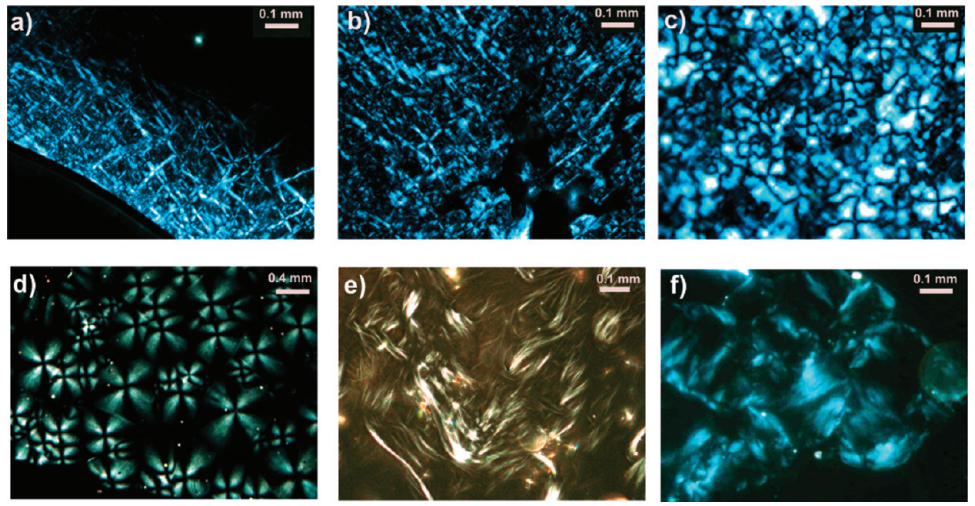

Figure 11. Representative PLM textures of mesophase of (a and b) Acryl-G2$^{gly-asp}$ 30%, (c) Acryl-G2$^{ala-asp}$ 10%, (d) Boc-G3$^{gly-asp}$ 40%, (e) Boc-G3$^{gly-asp}$ 8%, and (f) Boc-G3$^{ala-asp}$ 18% in benzyl alcohol.

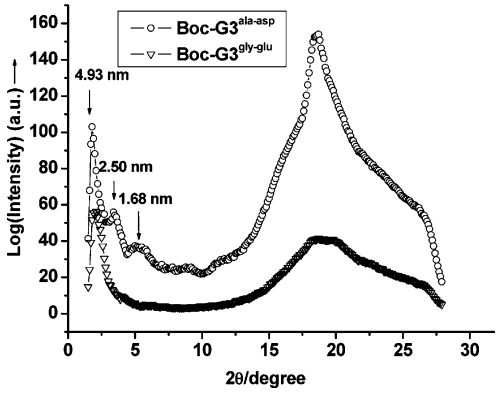

Figure 12. 1D WAXD patterns of Boc-G3$^{ala-asp}$ 18% and Boc-G3$^{gly-glu}$ 30% in benzyl alcohol.

self-assembly. Although both Acrylic-G2$^{gly-asp}$ and Acrylic-G2$^{ala-asp}$ dendrons were capable of forming lyotropic LCs in benzyl alcohol, the former displayed strong birefringence at concentrations exceeding 30 wt % (in benzyl alcohol) (Figure 11a and b), while the latter exhibited the lyotropic LC phase at concentrations as low as 10 wt % (Figure 11c).

CONCLUSION

In summary, we have conducted systematic studies on the structural changes of the dendritic branches, focal moieties, generation, and peripheral groups for their organogel and LC properties. The following conclusions can be draw: (1) Both organogel and LC properties of the amino acid-based dendrons subject to the dendritic effect. None of G1 dendrons could form mesophase structure in bulk or solvent; G2 dendrons showed versatile self-assembly ability depending on the building blocks in the dendritic branches and the focal group; G3 dendrons gelled organic solvents with the lowest critical gelation concentration (CGC) and self-organized into lyotropic LCs in benzyl alcohol. (2) Minor changes in the structures significantly affect their self-assembly behavior. Only the dendrons with a focal acrylic group, Acrylic-G2$^{gly-asp}$ and Acrylic-G2$^{ala-asp}$, could form both thermotropic and lyotropic LCs; the dendrons with carboxyl ends, Boc-G2-COOH, lost their self-assembly ability for being without the $\pi-\pi$ stacking interaction of phenyl groups; the dendrons with D-alanine as building blocks, Boc-G2$^{ala-asp}$, showed excellent properties both in organogel and LCs. Efforts are ongoing to construct novel peptide dendritic systems for addressing the ultrasound effect and chiral issue.

EXPERIMENTAL SECTION

General. All reagents and common solvents were obtained from commercial sources and used as received, except for special statements. ^{1}H NMR spectra were recorded on Bruker 400 MHz spectrometers at room temperature using d_6-dimethyl sulfoxide and $CDCl_3$ as solvents and tetramethylsilane as an internal standard. ^{13}C NMR spectra were recorded on Bruker 100 MHz spectrometers. Matrix-assisted laser desorption ionization time-of-flight (MALDI-TOF) mass-spectra were acquired on a BIFLE XIII time-of-flight MALDI mass spectrometer with α-cyano-4-hydroxycinnamic acid (CCA) as the matrix, which can give the best resolution. FTIR spectra were obtained using a Bruker VECTOR22 IR spectrometer. Tapping-mode atomic force microscopy (AFM) measurement was performed using a SPA-400 multimode AFM and SPI3800N probe station. For the preparation of AFM samples, the loose gel was dropped on a freshly cleaved mica surface and air-dried at room temperature before imaging. TEM was performed using a JEM-100 CXII microscope, operating at an acceleration voltage of 100 kV. Powder wide-angle X-ray diffraction (WAXD) patterns of xerogels were obtained using a Bruker D8 Discover diffractometer with GADDS as a 2D detector. Air scattering was subtracted from the sample patterns. Diffraction patterns were recorded in transmission mode at room temperature employing Cu Kα radiation. SAXS measurements were performed on equipment with a SAXSess camera (Anton-Paar, Graz Austria), which is connected with an X-ray generator (Philips) operating at 40 kV and 50 Ma employing Cu Kα radiation (λ = 0.154 nm). The 1D scattering function (log $I(q)$) was obtained by integrating the 2D scattering pattern, which was recorded on an imaging-plate detector (Perkin-Elmer) using SAXSQuant software (Anton-Paar, Graz Austria). Gel was naturally dried for two days at room temperature before the WAXD experiment. DSC measurements were carried out on a thermal analysis Q100 DSC system. Polarized light microscopy (PLM) was used to observe the LC textures of the samples on a Leitz Laborlux 12 microscope. The rheology was measured with a ThermoHaake RS300 rheometer.

ASSOCIATED CONTENT

Supporting Information

Characterization of Acrylic-G2$^{ala-asp}$ and Boc-G3$^{ala-asp}$, SAXS results of Boc-G2$^{ala-asp}$ and Acrylic-G2$^{ala-asp}$, DSC diagrams of

dx.doi.org/10.1021/cm201913p | Chem. Mater. 2012, 24, 71–80

liquid crystalline. This material is available free of charge via Internet at http://pubs.acs.org.

AUTHOR INFORMATION

Corresponding Author

*E-mail: xrjia@pku.edu.cn; eqchen@pku.edu.cn.

ACKNOWLEDGMENTS

This work is financially supported by the National Natural Science Foundation of China (20974004) and partially supported by the National Basic Research Program of China (973 Program, No. 2011CB933300) grant to X.R.J. We acknowledge Dr. Hai-Ming Fan and Professor De-Hai Liang at Peking University for their help with rheological studies.

REFERENCES

(1) (a) Jang, W. D.; Jiang, D. L.; Aida, T. *J. Am. Chem. Soc.* **2000**, *122*, 3232−3233. (b) Jang, W. D.; Aida, T. *Macromolecules* **2003**, *36*, 8461−8469.

(2) (a) Smith, D. K. *Adv. Mater.* **2006**, *18*, 2773−2278. (b) Hirst, A. R.; Smith, D. K. *Top. Curr. Chem.* **2005**, *256*, 237−273. (c) Smith, D. K. *Chem. Commun.* **2006**, 34−44.

(3) (a) Percec, V.; Cho, W. D.; Ungar, G.; Yeardley, D. J. P. *Chem.—Eur. J.* **2002**, *8*, 2011−2025. (b) Percec, V.; Glodde, M.; Peterca, M.; Rapp, A.; Schnell, I.; Spiess, H. W.; Bera, T. K.; Miura, Y.; Balagurusamy, V. S.; K. Aqad, E.; Heiney, P. A. *Chem.—Eur. J.* **2006**, *12*, 6298−6314. (c) Percec, V.; Won, B. C.; Peterca, M.; Heiney, P. A. *J. Am. Chem. Soc.* **2007**, *129*, 11265−11278.

(4) (a) Feng, Y.; Liu, Z. T.; Liu, J.; He, Y. M.; Zheng, Q. Y.; Fan, Q. H. *J. Am. Chem. Soc.* **2009**, *131*, 7950−7951. (b) Haridas, V.; Sharma, Y. K.; Creasey, R.; Sahu, S.; Gibson, C. T.; Voelcker, N. H. *New J. Chem.* **2011**, *35*, 303−309. (c) Liu, B.; Yang, J.; Yang, M. O.; Wang, Y. L.; Xia, N.; Zhang, Z. J.; Zheng, P.; Wang, W.; Lieberwirth, I.; Kubel, C. *Soft Matter* **2011**, *7*, 2317−2320.

(5) Hirst, A. R.; Huang, B. Q.; Castelletto, V.; Hamley, I. W.; Smith, D. K. *Chem.—Eur. J.* **2007**, *13*, 2180−2188.

(6) Duan, P. F.; Liu, M. H. *Langmuir* **2009**, *25*, 8706−8713.

(7) Palui, G.; Simon, F. X.; Schmutz, M.; Mesini, P. J.; Banerjee, A. *Tetrahedron* **2008**, *64*, 175−185.

(8) Baigude, H.; Katsuraya, K.; Okuyama, K.; Hatanaka, K.; Ikeda, E.; Shibata, N.; Uryu, T. *J. Polym. Sci., Part A: Polym. Chem.* **2004**, *42*, 1400−1414.

(9) Hirst, A. R.; Smith, D. K.; Feiters, M. C.; Geurts, H. P. M. *Chem.—Eur. J.* **2004**, *10*, 5901−5910.

(10) Hirst, A. R.; Smith, D. K. *Org. Biomol. Chem.* **2004**, *2*, 2965−2971.

(11) Chow, H. F.; Zhang, J. *Chem.—Eur. J.* **2005**, *11*, 5817−5831.

(12) (a) Donnio, B.; Buathong, S.; Bury, I.; Guillon, D. *Chem. Soc. Rev.* **2007**, *36*, 1495−1513. (b) Marcos, M.; Martin-Rapun, R.; Omenat, A.; Serrano, J. L. *Chem. Soc. Rev.* **2007**, *36*, 1889−1901. (c) Rosen, B. M.; Wilson, C. J.; Wilson, D. A.; Peterca, M.; Imam, M. R.; Percec, V. *Chem. Rev.* **2009**, *109*, 6275−6540.

(13) Tschierske, C. *Prog. Polym. Sci.* **1996**, *21*, 775−852.

(14) Percec, V.; Peterca, M.; Yurchenko, M. E.; Rudick, J. G.; Heiney, P. A. *Chem.—Eur. J.* **2008**, *14*, 909−918.

(15) Kamikawa, Y.; Kato, T. *Org. Lett.* **2006**, *8*, 2463−2466.

(16) Angelova, A.; Angelov, B.; Mutafchieva, R.; Lesieur, S.; Couvreur, P. *Acc. Chem. Res.* **2011**, *44*, 147−156.

(17) Ji, Y.; Luo, Y. F.; Jia, X. R.; Chen, E. Q.; Huang, Y.; Ye, C.; Wang, B. B.; Zhou, Q. F.; Wei, Y. *Angew. Chem., Int. Ed.* **2005**, *44*, 6025−6029.

(18) (a) Li, W. S.; Jia, X. R.; Wang, B. B.; Ji, Y.; Wei, Y. *Tetrahedron* **2007**, *63*, 8794−8800. (b) Kuang, G. C.; Ji, Y.; Jia, X. R.; Li, Y.; Chen, E. Q.; Wei, Y. *Chem. Mater.* **2008**, *20*, 4173−4175. (c) Kuang, G. C.; Ji, Y.; Jia, X. R.; Chen, E. Q.; Gao, M.; Yeh, J. M.; Wei, Y. *Chem. Mater.* **2009**, *21*, 456−462. (d) Kuang, G. C.; Teng, M. J.; Jia, X. R.; Chen, E. Q.; Wei, Y. *Chem.—Asian. J.* **2011**, *6*, 1163−1170.

(19) (a) Ji, Y.; Kuang, G. C.; Jia, X. R.; Chen, E. Q.; Wang, B. B.; Li, W. S.; Wei, Y.; Jiang, L. *Chem. Commun.* **2007**, 4233−4235. (b) Kuang, G. C.; Ji, Y.; Jia, X. R.; Li, Y.; Chen, E. Q.; Zhang, Z. X.; Wei, Y. *Tetrahedron* **2009**, *65*, 3496−3501.

(20) (a) Maity, S.; Kumar, P.; Haldar, D. *Soft Matter* **2011**, *7*, 5239−5245. (b) Wang, Y. B.; Zhan, C. L.; Fu, H. B.; Li, X.; Sheng, X. H.; Zhao, Y. S.; Xiao, D. B.; Ma, Y.; Yao, J. N. *Langmuir* **2008**, *24*, 7635−7638. (c) Li, Y. G.; Wang, T. Y.; Liu, M. H. *Tetrahedron* **2007**, *63*, 7468−7473.

(21) Love, C. S.; Hirst, A. R.; Chechik, V.; Smith, D. K.; Ashworth, I.; Brennan, C. *Langmuir* **2004**, *20*, 6580−6585.

(22) Hirst, A. R.; Coates, I. A.; Boucheteau, T. R.; Miravet, J. F.; Escuder, B.; Castelletto, V.; Hamley, I. W.; Smith, D. K. *J. Am. Chem. Soc.* **2008**, *130*, 9113−9121.

(23) Brizard, A.; Oda, R.; Huc, I. *Top. Curr. Chem.* **2005**, *256*, 167−218.

(24) (a) Yagai, S.; Higashi, M.; Karatsu, T.; Kitamura, A. *Chem. Mater.* **2005**, *17*, 4392−4398. (b) Yang, Z. M.; Liang, G. L.; Ma, M. L.; Gao, Y.; Xu, B. *Small* **2007**, *3*, 558−562. (c) Stokes, J. R.; Frith, W. J. *Soft Matter* **2008**, *4*, 1133−1140.

(25) Wang, C.; Zhang, D. Q.; Xiang, J. F.; Zhu, D. B. *Langmuir* **2007**, *23*, 9195−9200.

(26) Kim, C.; Kim, K. T.; Chang, Y.; Song, H. H.; Cho, T. Y.; Jeon, H. J. *J. Am. Chem. Soc.* **2001**, *123*, 5586−5587.

(27) Chow, H. F.; Wang, G. X. *Tetrahedron* **2007**, *63*, 7407−7418.

(28) Nagasawa, J.; Kudo, M.; Hayashi, S.; Tamaoki, N. *Langmuir* **2004**, *20*, 7907−7916.

(29) (a) Hirst, A. R.; Smith, D. K.; Feiters, M. C.; Geurts, H. P. M.; Wright, A. C. *J. Am. Chem. Soc.* **2003**, *125*, 9010−9011. (b) Huang, B. Q.; Hirst, A. R.; Smith, D. K.; Castelletto, V.; Hamley, I. W. *J. Am. Chem. Soc.* **2005**, *127*, 7130−7139.

(30) Hirst, A. R.; Smith, D. K. *Chem.—Eur. J.* **2005**, *11*, 5496−5508.

(31) Hudson, S. D.; Jung, H. T.; Percec, V.; Cho, W. D.; Johansson, G.; Ungar, G.; Balagurusamy, V. S. K. *Science* **1997**, *278*, 449−452.